Arab J Sci Eng (2016) 41:4799–4808
DOI 10.1007/s13369-016-2143-1

RESEARCH ARTICLE - CIVIL ENGINEERING

The Effect of Palm Oil Fuel Ash as a Supplementary Cementitious Material on Chloride Penetration and Microstructure of Blended Cement Paste

Wunchock Kroehong[1] · **Nattapong Damrongwiriyanupap**[2] · **Theerawat Sinsiri**[3] · **Chai Jaturapitakkul**[4]

Received: 15 April 2015 / Accepted: 14 April 2016 / Published online: 4 May 2016

Abstract This article presents the effect of palm oil fuel ash as a supplementary cementitious material on chloride penetration and microstructure of blended cement paste. Palm oil fuel ash (POFA) was ground to obtain two finenesses: one was the same size as the cement and the other was smaller than the cement. Type I ordinary Portland cement (OPC) was replaced by POFA at 0, 10, 20, 30, and 40 % by weight of binder. All paste specimens were prepared using the same water to binder ratio as 0.35. The compressive strength, pore size distribution, total chloride content, free chloride content, and X-ray diffraction analysis of chloride penetration into blended cement pastes were investigated. The results indicated that, at 60 and 90 days, the blended cement pastes containing 30 % of POFA with high fineness had 1.6 and 4.9 % higher compressive strength than that of the OPC paste, respectively. POFA pastes had a lower chloride diffusion coefficient and shallower concentration profile of free chloride than that of the OPC paste. The specimens containing coarse fineness and small particle size POFA had lower chloride diffusion coefficient than OPC paste ranging between 13.2 and 61.0 %. In addition, the chloride diffusion coefficient is linearly correlated with the critical pore diameters. Replacement of OPC by the fine-grained POFA resulted in the decrease in free chloride and in the chloride diffusion coefficient.

Keywords Palm oil fuel ash · Pozzolanic reaction · Chloride penetration · Chloride diffusion coefficient · Friedel's salt · Critical pore diameter

1 Introduction

The chloride-induced corrosion of embedded reinforcement is one of the most severe durability problems for concrete structures in a marine environment and exposed to deicing salts. Initially, steel embedded in concrete has a thin passive film on its surface that prevents the steel from further corroding. Chloride-induced corrosion begins when the concentration of chloride at the steel bars reaches a threshold value and then destroys the protective film layer [1–3]. This degradation mechanism leads to a series of structural problems, such as a reduction in the cross-sectional area of the reinforcement, cracking, delamination of the concrete cover, and weakening of the steel concrete bond, thereby reducing the load carrying capacity of the reinforced concrete structure [1–3]. To solve this problem, many supplementary cement materials (SCMs) have been suggested; for example, fly ash, ground granulated blast furnace slag, silica fume, and metakaolin have been found to be beneficial in resisting the ingress of chloride ions into concrete. This resistance is caused by the microstructure densification imparted by the pozzolanic reaction or secondary reaction from these materials. In addition, concrete containing pozzolans has a lower average pore size and critical pore size decreasing than that of control concrete [4]. The critical pore size is defined as

✉ Nattapong Damrongwiriyanupap
nattapong.da@up.ac.th

[1] Department of Civil Engineering, Faculty of Engineering and Architecture, Uthenthawai Campus, Rajamangala University of Technology Tawan-ok, Bangkok 10330, Thailand

[2] Civil Engineering Program, School of Engineering, University of Phayao, Phayao 56000, Thailand

[3] School of Civil Engineering, Institute of Engineering, Suranaree University of Technology, Nakhon Ratchasima 30000, Thailand

[4] Department of Civil Engineering, Faculty of Engineering, King Mongkut's University of Technology Thonburi, Bangkok 10140, Thailand

the inflection point on the cumulative pore volume and pore diameter plot or as the maximum of $dv/d(\log D)$. The critical pore size is the most frequent continuous pores [5].

Numerous studies have utilized by-product materials such as fly ash, rice husk ash, palm oil fuel ash, and bagasse ash as pozzolans to reduce the cement content in concrete mixtures. Palm oil fuel ash (POFA) is a by-product of palm oil factories, where palm shells, empty fruit bunches, and palm fiber are burnt as fuel at temperatures of 800–900 °C. More than 100,000 tons of POFA are produced every year in Thailand [6]. POFA is rarely utilized, and disposing of this waste may lead to future environmental problems. Previous researchers have studied the use of POFA as a partial replacement of cement in concrete. The results showed that POFA with a high fineness exhibits an excellent pozzolanic reaction and could be used as a supplementary material to produce high-strength concrete [7]. Later, Tangchirapat et al. [8] and Sinsiri et al. [9] found that ground POFA was a good pozzolanic material and could be used to replace Portland cement up to 30 % by weight of binder. In addition, the use of POFA can improve concrete strength and decrease water permeability [6]. Furthermore, the partial replacement of OPC with POFA assists in the sulfate [8] and chloride [10] penetration resistance of concrete. For microstructure of pastes, the critical pore size and average pore of blended cement paste containing POFA was lower than the OPC cement paste. The incorporation of high fineness POFA decreased the critical pore size and average pore of blended cement paste as compared to that with coarse POFA [5]. This effect is an important factor for decreasing permeability and chloride diffusion.

Previous studies have already reported the influence of POFA on compressive strength, chloride penetration, and microstructure of blended cement pastes. However, the relationship between chloride penetration and microstructure of blended cement pastes has not been well determined. If a by-product material from POFA can be used as a cement replacement in concrete, it will help to reduce energy due to decreasing the production of cement clinker and reducing the volume of waste disposed in landfills. In general, concrete and mortar can be considered as composite materials comprising of two phases, i.e., cement paste and aggregates. Many studies have shown that cement paste phase represents the main physical and mechanical property of concrete or mortar. For example, CSH is the principal binding agent in cement paste and is responsible for strength and shrinkage. Also, the porosity taking place in the concrete is mainly in cement paste phase which is the important property for diffusion mechanism related to durability of concrete. Thus, the objective of this research was to study the effect of palm oil fuel ash as a supplementary cementitious material on chloride penetration and microstructure of blended cement paste. The effect of ground palm oil fuel with two different finenesses on compressive strength, pore size distribution, total chloride content, free chloride content, X-ray diffraction analysis of chloride penetration of blended cement pastes was determined.

2 Experiments

2.1 Materials

The materials used in this study were type I ordinary Portland cement (OPC) and palm oil fuel ash (POFA). POFA was collected from thermal power plants in Thailand. The original POFA had large particles with low pozzolanic properties [7–11]. Thus, the original POFA was sieved through a sieve no. 16 to remove the large particles and any incompletely combusted material. Then, the POFA was ground to two different sizes. POFA was ground to have the same particle size as OPC for the first fineness (CPOFA). For the second fineness, the materials were ground to have particles that could act as fillers between the particles of cement (FPOFA). The physical properties of the materials are presented in Table 1. The specific gravity or density of OPC, CPOFA, and FPOFA was measured according to ASTM C188 and they were 3.14, 2.36, and 2.48, respectively. The Blaine fineness values of OPC, CPOFA, and FPOFA was evaluated following ASTM C204 2001 and they were 360, 670, and 1,490 m^2/kg, respectively. The median particle sizes of OPC, CPOFA, and FPOA were quantified using laser particle size analysis and they were 14.6, 15.6, and 2.1 μm, respectively. The chemical compositions of the materials are given in Table 2. SiO_2 is the major chemical component of CPOFA and FPOFA is 54.0 and 55.7 %, respectively. LOI and SO_3 are within the limits of 10.0 and 4 %, respectively. The total amounts of SiO_2, Al_2O_3, and Fe_2O_3 of CPOFA and FPOFA were 56.9 and 58.6 %, respectively, both of which are less than 70 %. A similar finding was also reported by other researchers and had a total SiO_2, Al_2O_3, and Fe_2O_3 content less than 70 % [12]. In general, the pozzolanic reaction takes place due to the reaction of $Ca(OH)_2$ with SiO_2 and Al_2O_3 existing in pozzolanic materials leading to the increase of calcium silicate hydrate (CSH). Thus, CPOFA and FPOFA with high

Table 1 Physical properties of the materials

Sample	Specific gravity	Median particle size (μm)	Blaine fineness (cm^2/g)
OPC	3.14	14.6	3,600
CPOFA	2.36	15.6	6,700
FPOFA	2.48	2.1	14,900

amount of SiO_2 tend to produce additional CSH in cement paste.

2.2 Mix Proportion

Ground POFA was used to partially replace type I Portland cement at the rates of 0, 10, 20, 30, and 40 % by weight of binder. The water to binder (W/B) ratio of 0.35 was used for all mixtures and is given in Table 3. To ensure homogeneity, the OPC and POFA were first mixed together for 3 min in the mixer, and then, the water was added. Afterward, the mixture was mixed for another 2 min. After mixing, the cement pastes were immediately cast into cube specimens of 50 × 50 × 50 mm. The cast specimens were covered with plastic to prevent water loss. After casting for 24 h, the specimens were removed from the molds and cured in saturated lime water at a temperature of 23 ± 2 °C.

2.3 Compressive Strength

The cube specimens of 50 × 50 × 50 mm were prepared in accordance with ASTM C 109 [13]. They were tested to determine the compressive strength at the ages of 7, 28, 60, and 90 days. Each compressive strength value reported is the average of five samples.

Table 2 Chemical compositions of the materials

Chemical composition (%)	OPC	CPOFA	FPOFA
Silicon dioxide (SiO_2)	20.8	54.0	55.7
Aluminum oxide (Al_2O_3)	4.7	0.9	0.9
Iron oxide (Fe_2O_3)	3.4	2.0	2.0
Calcium oxide (CaO)	65.3	12.9	12.5
Magnesium oxide (MgO)	–	4.9	5.1
Sodium oxide (Na_2O)	0.1	1.0	1.0
Potassium oxide (K_2O)	0.4	13.5	11.9
Sulfur trioxide (SO_3)	2.7	4.0	2.9
Loss on ignition (LOI)	0.9	3.7	4.7
$SiO_2 + Al_2O_3 + Fe_2O_3$	–	56.9	58.6

Table 3 Mixture proportions of the pastes

Mix no.	Symbol	OPC	CPOFA	FPOFA	W/B
1	OPC	100	–	–	0.35
2	10CPOFA	90	10	–	0.35
3	20CPOFA	80	20	–	0.35
4	30CPOFA	70	30	–	0.35
5	40CPOFA	60	40	–	0.35
6	10FPOFA	90	–	10	0.35
7	20FPOFA	80	–	20	0.35
8	30FPOFA	70	–	30	0.35
9	40FPOFA	60	–	40	0.35

2.4 Determination of the Porosity of the Pastes

In general, pore diameter distribution is the critical component of hydrated cement paste that strongly impacts on durability. In order to have low permeability and durable concrete, it is required to decrease pore diameter distribution. It is well known that the use of pozzolanic materials as a partial cement replacement can improve the pore diameter distribution of cement paste [5,14]. The pore diameter distribution in the hardened cement pastes was measured by mercury intrusion porosimetry (MIP) at a pressure capacity of 228 MPa. After curing for 90 days, the samples were split from the middle portion of the hardened blended cement paste. To stop the hydration reaction, the samples were submerged directly into liquid nitrogen for 5 min and were then evacuated at a pressure of 0.5 Pa at 40 °C for 48 h. This method has been used previously to stop the hydration reaction of cement paste [15,16]. The pressure is determined by the Washburn equation [17]. A constant contact angle of 140° and a constant surface tension of mercury of 480 mN/m were used for the pore size calculation.

2.5 Chloride Penetration Test

Specimens (100 mm diameter and 200 mm height) were prepared in accordance with ASTM C 39 [18] excepted that no sand was used in the mixture. The cast specimens were removed from the mold. Afterward, they were cured in saturated lime water at 23 ± 2 °C. After curing to the age of 27 days, they were cut into 60 mm pieces. The lateral and bottom surfaces of the cylinders were coated with epoxy. The samples were immersed in 3 % (0.513 mol/l) NaCl solution for 90 days as shown in Fig. 1; after that, the chloride penetra-

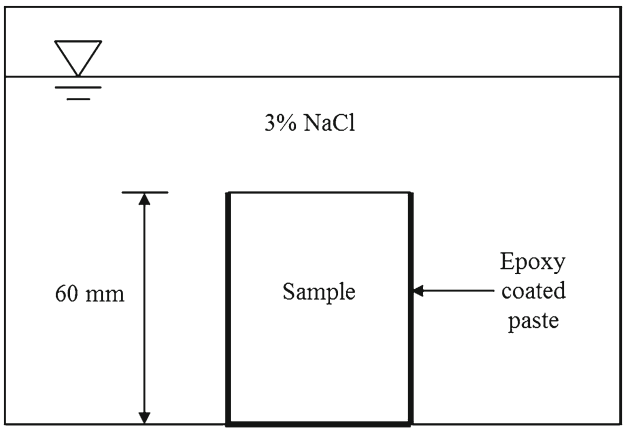

Fig. 1 Immersion of paste specimen in 3 % NaCl solution

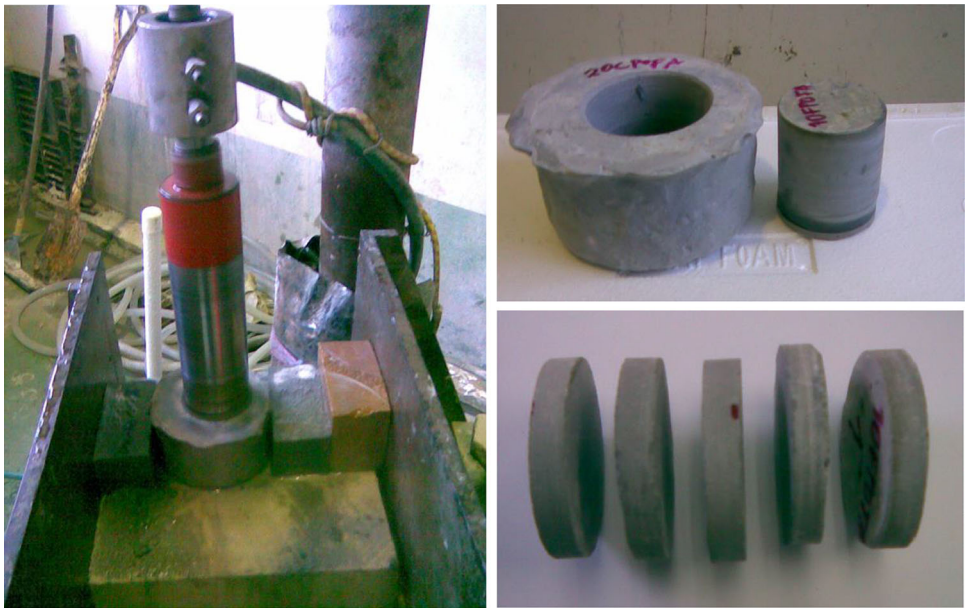

Fig. 2 Paste specimens coring and cutting for chloride test

tion into blended cement paste was measured. After 90 days of the chloride exposure period, the specimen was dry-cut from the top surface, which was 10 mm thick as shown in Fig. 2. The paste was ground into a powder sample that could pass through a No. 20 sieve. Nitric acid was mixed into the 10 g powder sample in a beaker, and the mixture was heated on a hot plate for 3 min. After removal of the beaker from the hot plate and filtering the solution, the filtrate was used to analyze the total chloride content using auto-titration equipment according to ASTM C1152 [19]. The method to determine the free chloride content is similar to that used for the total chloride content. 10 g of powder samples and distilled water were mixed in a beaker. The mixture was heated on the hot plate for 5 min, and then, the sample was left to stand for 24 h before filtering the solution. The filtrate was used to analyze the free chloride content using auto-titration equipment according to ASTM C 1218 [15].

2.6 Microstructure of the Blended Cement Paste After Chloride Penetration Test

After 90 days of the chloride exposure period, the specimen was dry-cut from the top surface, which was 10 mm thick. The paste was ground to a powder sample that could pass through a No. 200 sieve. The amount of Friedel's salt was determined using semiquantitative XRD. The XRD scans were performed for 2θ between 10° and 25° using an increment of 0.02°/step and a scan speed of 0.5 s/step. The mechanism of Friedel's salt formation is related to chemical process occurring in cement paste that chloride ions react with certain components of Portland cement producing chloride binding. Therefore, XRD allows determination the presence of Friedel's salt and helps to evaluate the bound chloride.

It is noted that, for all mechanical and physical tests at each curing time of different cement blends, at least five samples were tested under the same condition to check for consistency of the test. In most cases, the results under the same testing condition were reproducible with a low mean standard deviation, SD ($SD/\bar{x} < 10\,\%$, where $\bar{x}$ is mean value).

3 Results and Discussion

3.1 Compressive Strength

The compressive strengths of paste samples at 7, 28, 60, and 90 days are given in Table 4. At 7 and 28 days, the compressive strengths of the pastes with 10–40 % POFA replacement are lower than that of OPC paste. At 90 days, the normalized compressive strengths of 10CPOFA, 20CPOFA, 30CPOFA, and 40CPOFA pastes are 105.4, 102.9, 98.0, and 88.9 % respectively. This means 10CPOFA and 20CPOFA samples exhibit higher strength while 30CPOFA and 40CPOFA pastes gain lower strength as compared to OPC paste. The effect of POFA fineness on strength development is evident at 28, 60, and 90 days. After 28 days, the normalized strengths of 10FPOFA and 20FPOFA, 105.7 and 103.1 %, are found to be higher than OPC sample, while the strength gain of 30FPOFA specimens is observed at 60 and 90 days. It is also obviously noticed that the compressive strength of 30FPOFA at 60 and 90 days is higher than those of 10CPOFA at 28 days. This was confirmed from the previous study [5] that the compressive strength of cement paste was significantly improved with high fineness POFA replacement. However, when using high amount of FPOFA replacement there is no evidence on

Table 4 Compressive strengths of the pastes

Symbol	Compressive strength (MPa)				Normalized compressive strength (%)			
	7 days	28 days	60 days	90 days	7 days	28 days	60 days	90 days
OPC	53.0	75.0	84.6	99.1	100.0	100.0	100.0	100.0
10CPOFA	51.3	74.8	86.3	104.5	96.8	99.7	101.6	105.4
20CPOFA	48.3	72.0	84.6	102.0	91.1	96.0	99.6	102.9
30CPOFA	44.5	66.7	78.6	97.1	84.0	88.9	92.9	98.0
40CPOFA	41.0	61.5	72.8	88.1	77.4	82.0	85.7	88.9
10FPOFA	53.7	79.3	93.3	111.3	101.3	105.7	109.9	112.3
20FPOFA	51.9	77.3	92.2	109.6	97.9	103.1	108.6	110.6
30FPOFA	48.3	72.8	86.3	104.0	91.1	96.9	101.6	104.9
40FPOFA	44.0	66.5	78.6	94.1	83.0	88.7	92.6	95.0

strength gain of the pastes as seen on 40FPOFA samples at all ages.

It can be concluded from the compressive strength results as given in Table 4 that the compressive strength of blended cement pastes increases with increasing of age but decreases with the increase in ash replacement. However, at the early age, the cement pastes containing POFA have lower compressive strength than that of OPC sample due to the dilution effect and low pozzolanic reaction [20]. Previous studies [16,17,21] have shown that the compressive strength of blended cement pastes can be improved by three features: the hydration reaction, the pozzolanic reaction, and the filler effect. The hydration reaction is related to the amount of cement in the mixture. The filler effect comprises of two phenomena that is the nucleation and packing effects depending mainly on the fineness of materials. The nucleation effect takes place when the small particles are spread in blended cement paste leading to enhance the hydration reaction while packing effect occurs when the voids in pastes are filled with fine particles. Thus, to enhance the strength of blended cement pastes, high fineness of biomass ash is suggested to be used that pastes become more homogeneous and denser. In addition to filler effect, the use of biomass ash in cement paste causes pozzolanic reaction. This process produces an additional calcium silicate hydrate (CSH) due to the reactivity of SiO_2 and Al_2O_3 contained in the biomass ash and $Ca(OH)_2$. The results obtained from this study are similar to other studies [22,23] that the optimum replacement of Portland cement type I by rice husk ash (RHA) and POFA is found to be 30 % by weight of binder and it does not weaken the compressive strength of pastes when the cement replacement is not greater than 30 %.

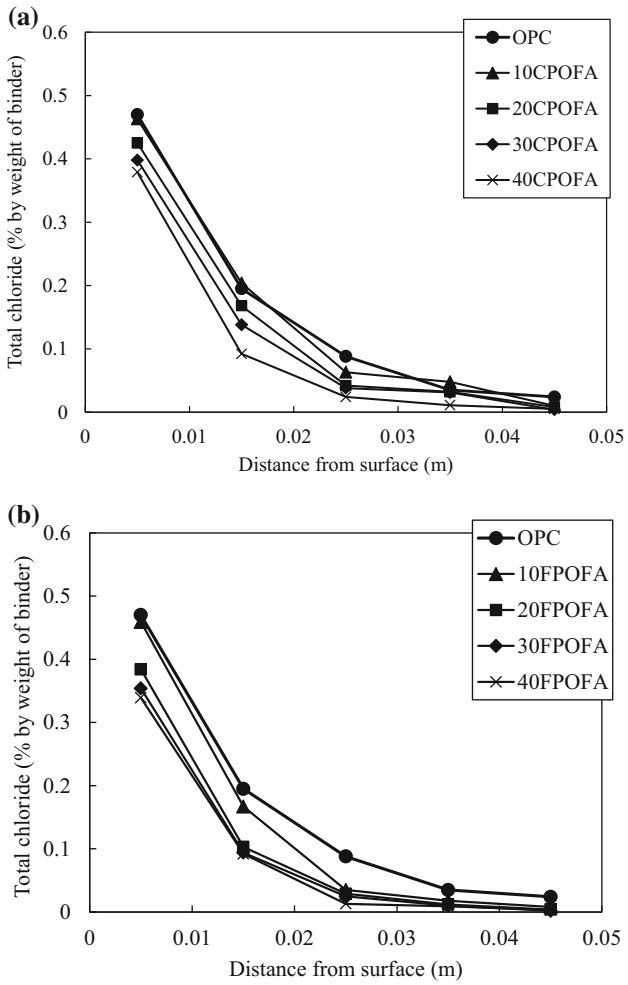

Fig. 3 Chloride penetration profile of OPC paste and FPOFA pastes at 90 days immersion in 3 % NaCl solution. **a** Coarse palm oil fuel ash (CPOFA), **b** fine palm oil fuel ash (FPOFA)

3.2 Effect of Palm Oil Fuel Ash on the Chloride Penetration Profiles

Figure 3 shows chloride penetration profile of OPC paste and POFA pastes at 90 days immersion in 3 % NaCl solution. The results showed that both CPOFA and FPOFA pastes had lower chloride contents than the OPC paste. In addition, the chloride content decreased with increasing replacement with POFA. This is due to physical adsorption on the surface of

the hydration or pozzolanic reaction product, such as C–S–H, C–A–H, ettringite, and monosulfate [24,25]. The effect of POFA fineness shows that the chloride penetration of FPOFA paste was lower than that of CPOFA paste. This is due to the paste with high fineness POFA having a lower total porosity than the coarse POFA. These results agree with Chindaprasirt et al. [26].

3.3 Effect of Palm Oil Fuel Ash on the Chloride Diffusion Coefficient

The chloride diffusion coefficient (D_c) was evaluated based on the general solution of Fick's second law of diffusion as given in Eq. (1).

$$C(x,t) = C_0\left[1 - \mathrm{erf}\left(\frac{x}{2\sqrt{D_c t}}\right)\right] \quad (1)$$

where $C(x,t)$ is the total chloride concentration (% by weight of binder) at depth x and exposure time t, C_o is the surface chloride concentration, t is time (s), x is distance from the top surface of sample (m), D_c is diffusion coefficient (m^2/s) at exposure time t, and erf is error function. The determination of D_c can be evaluated by fitting the Fick's second law on chloride concentration profile of the specimen from experiments. Figure 4 shows the fitting curve of the general solution of Fick's second law of pastes at 90 days immersion in 3 % NaCl solution. After the chloride concentration at paste surface (C_o) was obtained that each regression has its own C_o value, the regression analysis yielded the chloride diffusion coefficient (D_c) at 90 days immersion in 3 % NaCl solution. For the same procedure, the values of D_c and C_o could be evaluated in the other paste mixtures.

The effects of palm oil fuel ash on the chloride diffusion coefficients of blended cement pastes are shown in Fig. 4. For coarse fineness palm oil fuel ash, the chloride diffusion coefficients of 10CPOFA, 20CPOFA, 30CPOFA, and 40CPOFA pastes were 13.8×10^{-12}, 11.6×10^{-12}, 9.7×10^{-12}, and 7.1×10^{-12} m^2/s, respectively, while that of OPC paste was 15.9×10^{-12} m^2/s. For the pastes with a small particle size, the chloride diffusion coefficients of the 10FPOFA, 20FPOFA, 30FPOFA, and 40FPOFA pastes were 11.1×10^{-12}, 8.1×10^{-12}, 7.2×10^{-12}, and 6.2×10^{-12} m^2/s. The results showed that the use of POFA to replace Portland cement type I had a lower chloride diffusion coefficient than the OPC paste. In addition, the chloride diffusion coefficients decreased with increasing fineness and an increase in the replacement rate of ash. This relationship is due to the pozzolanic reaction in palm oil fuel ash pastes. Thus, the pore size distribution in the blended cement pastes was refined. The small particles fill the voids of the paste [17,21,27,28].

Figure 5 shows the effect of palm oil fuel ash fineness on the chloride diffusion coefficient of blended cement paste at

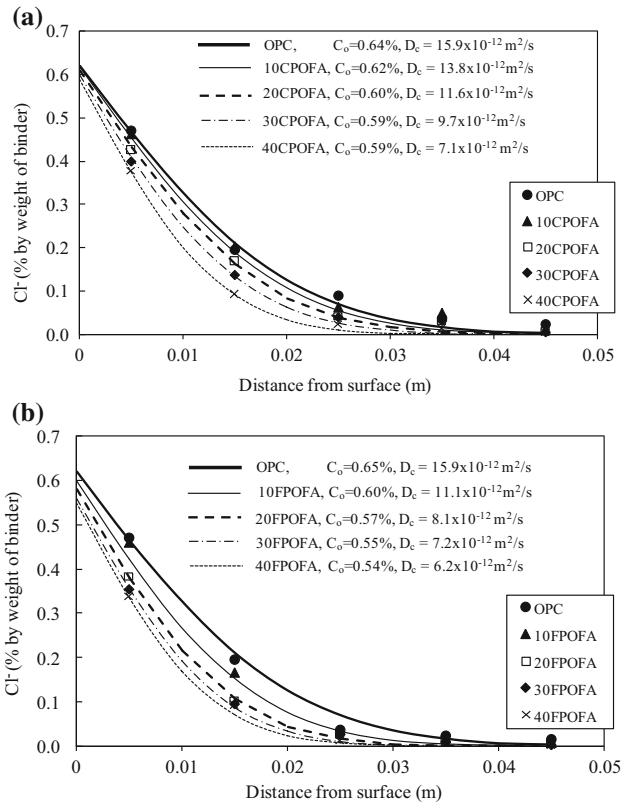

Fig. 4 Chloride diffusion coefficients of OPC paste and POFA pastes at 90 days immersion in 3 % NaCl solution. **a** Coarse palm oil fuel ash (CPOFA), **b** fine palm oil fuel ash (FPOFA)

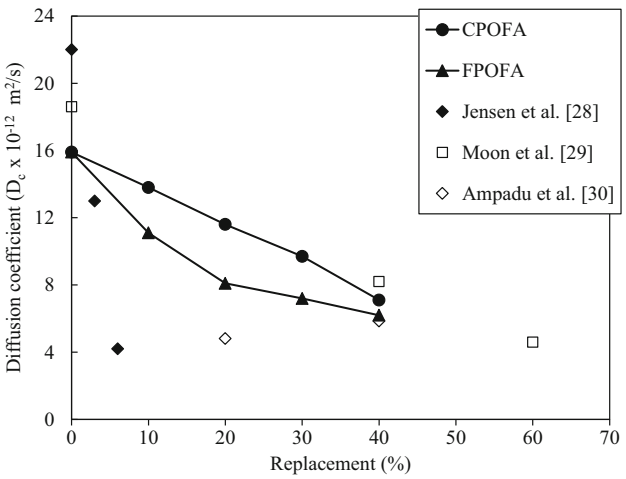

Fig. 5 Effect of POFA on the chloride diffusion coefficients of blended cement paste at 90 days immersion in 3 % NaCl solution

90 days immersion in 3 % NaCl solution. The chloride diffusion coefficients of blended cement paste containing 3 and 6 % of silica fume from Jensen et al. [29] are also plotted in Fig. 5 and compared with the trended line of POFA paste. The data from Jensen et al. [29] are lower than those of the POFA paste. The data of Moon et al. [30] and Ampadu et al. [31] are

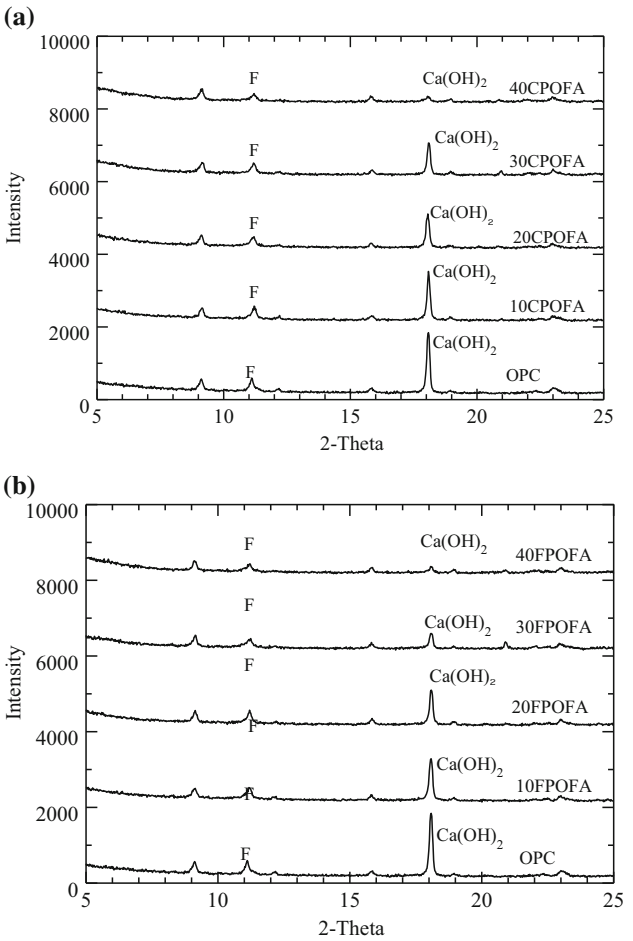

Fig. 6 X-ray diffraction patterns of pastes at 90 days immersion in 3 % NaCl solution F = Friedel's salt. **a** Coarse palm oil fuel ash (CPOFA), **b** fine palm oil fuel ash (FPOFA)

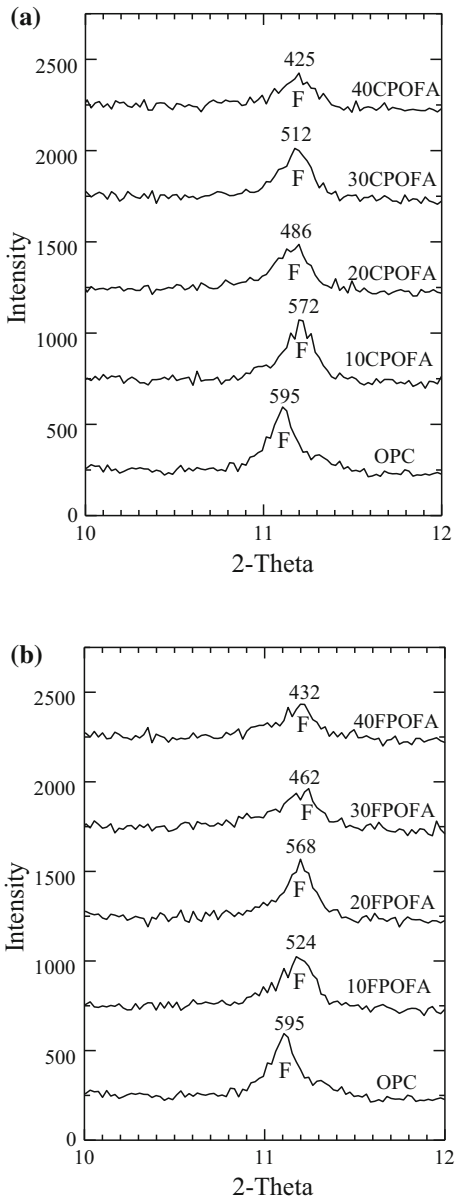

Fig. 7 X-ray diffraction patterns of Friedel's salt in pastes at 90 days immersion in 3 % NaCl solution F = Friedel's salt. **a** Coarse palm oil fuel ash (CPOFA), **b** fine palm oil fuel ash (FPOFA)

also plotted that the chloride diffusion coefficients of blended cement paste containing fly ash obtained from Ampadu et al. [31] are slightly lower than that of the POFA paste, while the chloride diffusion coefficients of concrete containing ground granulated blast furnace slag obtained from Moon et al. [30] are close to the trend line of the POFA paste. It is also evident from Fig. 5 that the chloride diffusion coefficient of cement paste decreases with higher amount of CPOFA and FPOFA replacement. The results confirm that the use of pozzolanic materials to replace Portland cement type I can provide a lower chloride diffusion coefficient than OPC paste.

3.4 X-ray Diffraction Analysis of Blended Cement Paste After Chloride Penetration

Figure 6 shows the X-ray diffraction patterns of pastes at 90 days immersion in 3 % NaCl solution. The peak intensity at 2-theta of Friedel's salt and $Ca(OH)_2$ were 11.2° and 18.0°, respectively. Generally, chloride binding capacity in concrete depends on chemically and physically bound chloride.

Chemically bound chloride is a reaction between chloride and tricalcium aluminate (C_3A) to form calcium chloroaluminate $3CaO{\cdot}Al_2O_3{\cdot}CaCl_2{\cdot}10H_2O$, which is called Friedel's salt. The X-ray diffraction patterns of Friedel's salt in pastes at 90 days immersion in 3 % NaCl solution are shown in Fig. 7. The results showed that POFA paste had a lower peak intensity of Friedel's salt than the OPC paste. Increase in the POFA to replace type I Portland cement resulted in low C_3A, leading to a low peak intensity of Friedel's salt from chemically bound chloride. In addition, POFA had a low Al_2O_3 content of 0.9 %. The previous research had reported that the amount of chloride binding increases with the alu-

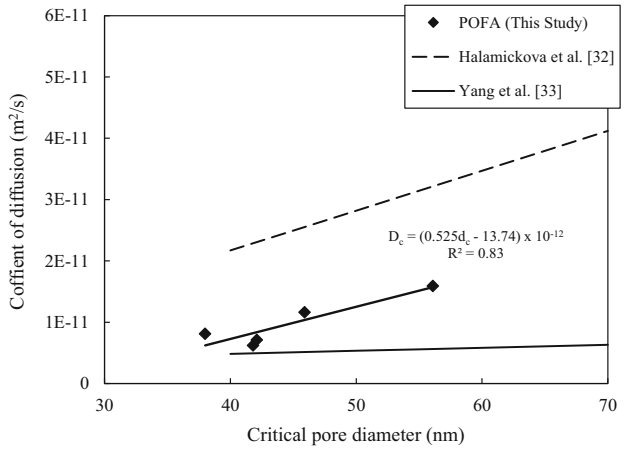

Fig. 8 Relationship between the chloride diffusion coefficient and critical pore diameters of blended cement paste

mina content of the pozzolanic materials [32]. As seen from Fig. 6, the peak intensity of $Ca(OH)_2$ decreases with increasing fineness of the POFA and POFA replacement of cement, resulting in the increase of C–S–H, C–A–S–H, and C–A–H. This is related to the absorption of chlorides that chlorides can be physically adsorbed by surface hydration and the pozzolanic reaction [24,25]. Thus, the increased use of POFA as a replacement for cement resulted in an increase in physically bound chloride.

3.5 Relationship Between the Chloride Diffusion Coefficient and Critical Pore Diameters of Blended Cement Pastes

Figure 8 shows the relationship between the chloride diffusion coefficient and the critical pore diameters of blended cement pastes. It can be seen that the critical pore diameter increases proportionally with the chloride diffusion coefficient. Previous research had reported that the relationship between the chloride diffusion coefficient and critical pore diameters was linearly correlated and increased with an increase in the critical pore diameter [33,34]. The equation to predict the chloride diffusion coefficient of blended cement paste related to critical pore is proposed as:

$$D_c = (0.525d_c - 13.74) \times 10^{-12} \quad (2)$$

where D_c is the chloride diffusion coefficient (10^{-12} m^2/s) and d_c is the critical pore diameter (nm). The correlation value of 0.83 indicates a strong linear relationship between the chloride diffusion coefficient and critical pore diameter.

The data of Halamickova et al. [33] and Yang et al. [34] studies are plotted in Fig. 8. It is noticed that the results from Halamickova et al. [33] are higher than the trend line, whereas the chloride diffusion coefficient and critical pore diameters of concrete obtained from Yang et al. [34] study are lower than the trend line. The distinct relationship of the trend lines is due to the different test methods and water cement ratios used to analyze the chloride diffusion coefficient. In Halamickova et al. [33] study, mortars of two water cement ratios, 0.4 and 0.5, were used and the chloride diffusion coefficients were determined by ASTM C 1202, the test method for electrical indication of concrete's ability to resist chloride ion penetration, while Yang et al. [34] conducted the 90-day ponding test following ASTM C 1543 to evaluate the chloride diffusion coefficient with eight water cement ratios of concrete and mortar specimens ranging from 0.3 to 0.65.

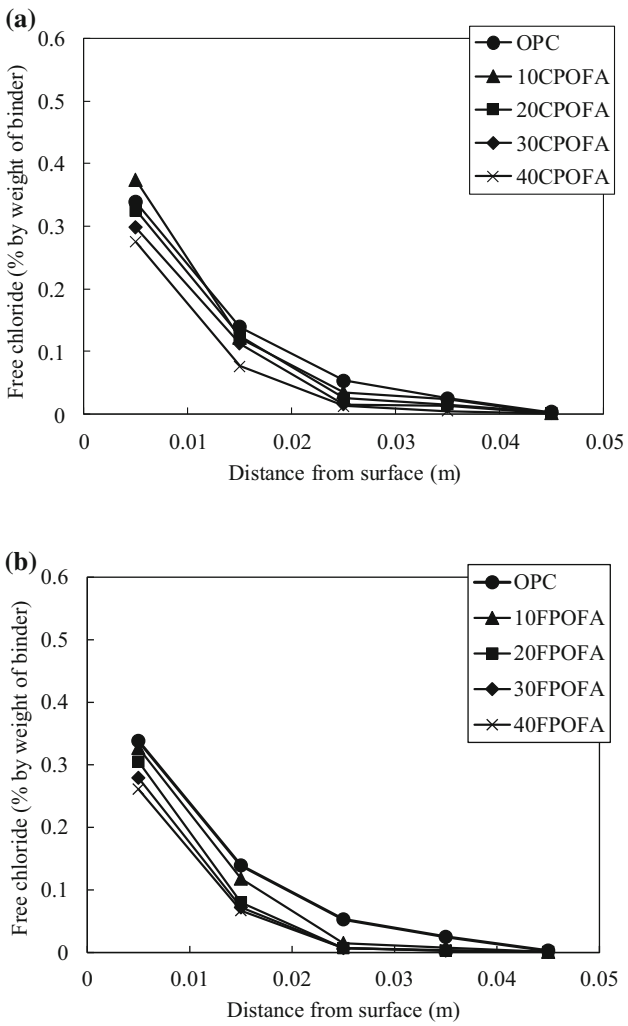

Fig. 9 Concentration profile of free chloride of OPC paste and POFA paste at 90 days immersion in 3 % NaCl solution. **a** Coarse palm oil fuel ash (CPOFA), **b** fine palm oil fuel ash (FPOFA)

3.6 Concentration Profiles of Free Chloride

Figure 9 shows the concentration profiles of free chloride of OPC paste and POFA paste at 90 days immersion in 3 %

NaCl solution. These results show that the penetration depth free chloride decreases with an increase in the replacement and fineness of POFA. In addition, the concentration of the POFA paste decreases with an increase in depth from the top surface. This result is due to increased physical sorption of chloride at lower chloride concentrations on the surface of hydration or pozzolanic reaction products, such as C–S–H, C–A–H, ettringite, and monosulfate and increased tortuosity, both resulting in decreased diffusion. Furthermore, the previous research [5,35] had reported that the critical pore size of the paste with pozzolanic materials was smaller than that of the OPC cement paste which was the most important factor for permeability and chloride ion diffusion [33,36]. These results illustrate that the use of palm oil fuel ash to replace OPC can provide a desirable concentration profile of free chloride.

4 Conclusions

The results of this study provide the following conclusions.

(1) The use of palm oil fuel ash with particle sizes smaller than that of OPC to replace Portland cement type I at the rate of 30 % by weight of binder resulted in good compressive strength between 86.3 and 104.0 MPa due to the filler effect and pozzolanic reaction.
(2) The use of palm oil fuel ash led to a lower chloride diffusion coefficient and reduced depth of the concentration profile of free chloride than the OPC paste. In addition, the chloride diffusion coefficient was positively correlated with the critical pore diameter.
(3) The increase in fineness and replacement of cement with palm oil fuel ash contributed to the decrease in free chloride and the chloride diffusion coefficient.
(4) The use of palm oil fuel ash to replace Portland cement type I had a lower peak intensity of Friedel's salt in paste than that of the OPC paste. In addition, the peak intensity of Friedel's salt in paste decreased with increasing replacement of POFA. However, increasing the replacement of cement by palm oil fuel ash resulted in high tortuosity, slower chloride diffusion, and lower chloride concentration. This led to lower pore water concentration and increasing of physically bound chloride.

Acknowledgments The authors would like to acknowledge the financial support of the Commission on Higher Education of Thailand for a grant under the Strategic Scholarships for Frontier Research Network for the Joint Ph.D. Program, Thai Doctoral degree. They also thank the Thailand Research Fund (TRF) for the financial support under the TRF Senior Research Scholar, Grant Nos. RTA5380002 and RTA5780004, and the TRF New Researcher Scholar, Grant Nos. TRG5880064 and MRG5580222.

References

1. Bastidas-Arteaga, E.; Chateauneuf, A.; Sanchez-Silva, M.; Bressolette, P.; Schoefs, F.: A comprehensive probabilistic model of chloride ingress in unsaturated concrete. Eng. Struct. **33**(3), 720–730 (2011)
2. Marsavina, L.; Audenaert, K.; De Schutter, G.; Faur, N.; Marsavina, D.: Experimental and numerical determination of the chloride penetration in cracked concrete. Constr. Build. Mater. **23**(1), 264–274 (2009)
3. Martin-Perez, B.; Zibara, H.; Hooton, R.D.; Thomas, M.D.A.: A study of the effect of chloride binding on service life predictions. Cem. Concr. Res. **30**(8), 1215–1223 (2000)
4. Li, Z.; Ding, Z.: Property improvement of Portland cement by incorporating with metakaolin and slag. Cem. Concr. Res. **33**(4), 579–584 (2003)
5. Kroehong, W.; Sinsiri, T.; Jaturapitakkul, C.; Chindaprasirt, P.: Effect of palm oil fuel ash fineness on the microstructure of blended cement paste. Constr. Build. Mater. **25**(11), 4095–4104 (2011)
6. Chindaprasirt, P.; Homwuttiwong, S.; Jaturapitakkul, C.: Strength and water permeability of concrete containing palm oil fuel ash and rice husk-bark ash. Constr. Build. Mater. **21**(7), 1492–1499 (2007)
7. Sata, V.; Jaturapitakkul, C.; Kiattikomol, K.: Utilization of palm oil fuel ash in high-strength concrete. J. Mater. Civ. Eng. **16**(6), 623–628 (2004)
8. Tangchirapat, W.; Jaturapitakkul, C.; Kiattikomol, K.: Compressive strength and expansion of blended cement mortar containing palm oil fuel ash. J. Mater. Civ. Eng. **21**(8), 426–431 (2009)
9. Sinsiri, T.; Kroehong, W.; Jaturapitakkul, C.; Chindaprasirt, P.: Assessing the effect of biomass ashes with different finenesses on the compressive strength of blended cement paste. Mater. Des. **42**, 424–433 (2012)
10. Chindaprasirt, P.; Rukzon, S.; Sirivivatnanon, V.: Effect of carbon dioxide on chloride penetration and chloride ion diffusion coefficient of blended Portland cement mortar. Constr. Build. Mater. **22**(8), 1701–1707 (2008)
11. Rukzon, S.; Chindaprasirt, P.; Mahachai, R.: Effect of grinding on chemical and physical properties of rice husk ash. Int. J. Miner. Metals Mater. **16**(2), 242–247 (2009)
12. Awal, A.S.M.A.; Hussin, M.W.: The effectiveness of palm oil fuel ash in preventing expansion due to alkali–silica reaction. Cem. Concr. Compos. **19**(4), 367–372 (1997)
13. ASTM C109 A: Standard Test Method for Compressive Strength of Hydraulic Cement Mortars (Using 2-in. or [50 mm] Cube Specimens). Annual Book of ASTM Standards, vol. 04.01 (2001)
14. Chindaprasirt, P.; Jaturapitakkul, C.; Sinsiri, T.: Effect of fly ash fineness on compressive strength and pore size of blended cement paste. Cem. Concr. Compos. **27**, 425–428 (2005)
15. ASTM C1218 A: Standard Test Method for Water-Soluble Chloride in Mortar and Concrete. Annual Book of ASTM Standards, vol. 04.02 (2001)
16. Cyr, M.; Lawrence, P.; Ringot, E.: Efficiency of mineral admixtures in mortars: quantification of the physical and chemical effects of fine admixtures in relation with compressive strength. Cem. Concr. Res. **36**(2), 264–277 (2006)
17. Gopalan, M.K.: Nucleation and pozzolanic factors in strength development of class F fly ash concrete. ACI Mater. J. **90**(2), 117–121 (1993)
18. ASTM C39 A: Standard Test Method for Compressive Strength of Cylindrical Concrete Specimens. Annual Book of ASTM Standards, vol. 04.02 (2001)
19. ASTM C1152 A: Standard Test Method for Acid-Soluble Chloride in Mortar and Concrete. Annual Book of ASTM Standards, vol. 04.02 (2001)

20. Zeyad, A.M.; Johari, M.A.M.; Bunnori, N.M.; Ariffin, K.S.; Altwair, N.M.: Characteristics of treated palm oil fuel ash and its effects on properties of high strength concrete. Adv. Mater. Res. **626**, 152–156 (2012)
21. Montgomery, D.G.; Hughes, D.C.; Williams, R.I.T.: Fly ash in concrete—a microstructure study. Cem. Concr. Res. **11**(4), 591–603 (1981)
22. Jaturapitakkul, C.; Tangpagasit, J.; Songmue, S.; Kiattikomol, K.: Filler effect and pozzolanic reaction of ground palm oil fuel ash. Constr. Build. Mater. **25**(11), 4287–4293 (2011)
23. Ganesan, K.; Rajagopal, K.; Thangavel, K.: Rice husk ash blended cement: assessment of optimal level of replacement for strength and permeability properties of concrete. Constr. Build. Mater. **22**(8), 1675–1683 (2008)
24. Luo, R.; Cai, Y.; Wang, C.; Huang, X.: Study of chloride binding and diffusion in GGBS concrete. Cem. Concr. Res. **33**(1), 1–7 (2003)
25. Sumranwanich, T.; Tangtermsirikul, S.: A model for predicting time-dependent chloride binding capacity of cement-fly ash cementitious system. Mater. Struct. **37**(6), 387–396 (2004)
26. Chindaprasirt, P.; Jaturapitakkul, C.; Sinsiri, T.: Effect of fly ash fineness on compressive strength and pore size of blended cement paste. Cem. Concr. Compos. **27**(4), 425–428 (2005)
27. Isaia, G.C.; Gastaldini, A.L.G.; Moraes, R.: Physical and pozzolanic action of mineral additions on the mechanical strength of high-performance concrete. Cem. Concr. Compos. **25**(1), 69–76 (2003)
28. Mehta, P.K; Aietcin, P-.C.C.: Principles underlying production of high-performance concrete. Cem. Concr. Aggreg. **12**(2), 70–78 (1990)
29. Jensen, O.M.; Hansen, P.F.; Coats, A.M.; Glasser, F.P.: Chloride ingress in cement paste and mortar. Cem. Concr. Res. **29**(9), 1497–1504 (1999)
30. Moon, H.Y.; Kim, H.S.; Choi, D.S.: Relationship between average pore diameter and chloride diffusivity in various concretes. Constr. Build. Mater. **20**(9), 725–732 (2006)
31. Ampadu, K.O.; Torii, K.; Kawamura, M.: Beneficial effect of fly ash on chloride diffusivity of hardened cement paste. Cem. Concr. Res. **29**(4), 585–590 (1999)
32. Thomas, M.D.A.; Hooton, R.D.; Scott, A.; Zibara, H.: The effect of supplementary cementitious materials on chloride binding in hardened cement paste. Cem. Concr. Res. **42**(1), 1–7 (2012)
33. Halamickova, P.; Detwiler, R.J.; Bentz, D.P.; Garboczi, E.J.: Water permeability and chloride ion diffusion in Portland cement mortars: relationship to sand content and critical pore diameter. Cem. Concr. Res. **25**(4), 790–802 (1995)
34. Yang, C.C.; Cho, S.W.; Wang, L.C.: The relationship between pore structure and chloride diffusivity from ponding test in cement-based materials. Mater. Chem. Phys. **100**(2–3), 203–210 (2006)
35. Poon, C.S.; Lam, L.; Kou, S.C.; Wong, Y.L.; Wong, R.: Rate of pozzolanic reaction of metakaolin in high-performance cement pastes. Cem. Concr. Res. **31**(9), 1301–1306 (2001)
36. Yang, C.C.: On the relationship between pore structure and chloride diffusivity from accelerated chloride migration test in cement-based materials. Cem. Concr. Res. **36**(7), 1304–1311 (2006)